Groundwater flow processes and mixing in active volcanic systems: The case of Guadalajara (Mexico)

A. Hernández-Antonio[1], J. Mahlknecht[1,*], C. Tamez-Meléndez[1], J. Ramos-Leal[2], A. Ramírez-Orozco[1], R. Parra[1], N. Ornelas-Soto[1], C.J. Eastoe[3]

[1]Centro del Agua para América Latina y el Caribe, Tecnológico de Monterrey
[2]División de Geociencias Aplicadas, Instituto Potosino de Investigación Científica y Tecnológica
[3] Department of Geosciences, University of Arizona

Abstract:

Groundwater chemistry and isotopic data from 40 production wells in the Atemajac and Toluquilla Valleys, located in and around the Guadalajara metropolitan area, were determined to develop a conceptual model of groundwater flow processes and mixing. Stable water isotopes (δ^2H, $\delta^{18}O$) were used to trace hydrological processes and tritium (^3H) to evaluate the relative contribution of modern water in samples. Multivariate analysis including cluster analysis and principal component analysis were used to elucidate distribution patterns of constituents and factors controlling groundwater chemistry. Based on this analysis, groundwater was classified into four groups: cold groundwater, hydrothermal water, polluted groundwater and mixed groundwater. Cold groundwater is characterized by low temperature, salinity, and Cl and Na concentrations and is predominantly of Na-HCO_3 type. It originates as recharge at Primavera caldera and is found predominantly in wells in the upper Atemajac Valley. Hydrothermal water is characterized by high salinity, temperature, Cl, Na, HCO_3, and the presence of minor elements such as Li, Mn and F. It is a mixed HCO_3 type found in wells from Toluquilla Valley and represents regional flow circulation through basaltic and andesitic rocks. Polluted groundwater is characterized by elevated nitrate and sulfate concentrations and is usually derived from urban water cycling and subordinately from agricultural return flow. Mixed groundwaters between cold and hydrothermal components are predominantly found in the lower Atemajac Valley. Most groundwater contains at least a small fraction of modern water. The application of a multivariate mixing model allowed to evaluate the mixing proportions of hydrothermal fluids, polluted waters and cold groundwater in sampled water. This study may help local water authorities to identify and dimension groundwater contamination, and act accordingly.

* Corresponding author: Jürgen Mahlknecht, Centro del Agua para América Latina y el Caribe, Tecnológico de Monterrey, Ave. Eugenio Garza Sada No. 2501, C.P. 64849 Monterrey, Nuevo León, México. E-mail: jurgen@itesm.mx

1 Introduction

Active volcanic systems are frequently accompanied by an intense hydrothermal circulation, which is controlled by the exchange of mass and energy between groundwater systems, magmatic fluids and hot rock (Goff and Janik, 2000; Di Napoli et al., 2009). The characterization of such hydrothermal systems helps on the one hand to quantify its geothermal energy potential and, on the other hand, to assess volcanic-related risks (Di Napoli et al., 2011). Hot springs, mud deposits, fumaroles, vaporization and degassing soils give initial clues about subsurface hydrothermal conditions (Hockstein and Browne, 2000; Navarro et al., 2011). The chemical characterization of fluids and groundwater has been used as an indicator of the subsurface structure and the origin of released fluids when hydrogeological information is scarce (Henley and Ellis, 1983; Appelo and Postma, 2005). Hydrochemical data, such as high electrical conductivity (EC), high temperatures and elevated concentrations of As, B, Br, Cl, Cs, F, Fe, Ge, I, Li, Mn, Mo, Na, Rb, Sb, Ta, U and W denote the presence of hydrothermal fluids in groundwater (Reimann et al. 2003; Dogdu and Bayari, 2005; Aksoy et al. 2009). However, hydrothermal volcanic systems are sometimes difficult to analyse due to the fact that groundwater is a mixture of fluids from various sources, sometimes consisting of shallow meteoric waters from recent infiltration, seawater and hot water rising from deep hydrothermal reservoirs (Chiodini et al., 2001; Evans et al, 2002; Di Napoli et al., 2009).

The combination of different environmental tracer techniques helps elucidate the groundwater´s origin, recharge, flow velocity and direction, residence or travel times, connections between aquifers, and surface and groundwater interrelations (Edmunds and Smedley 2000; De Vries and Simmers 2002; Appello and Postma, 2005; Ako et al., 2013; Stumpp et al., 2014). These techniques have been applied in large semiarid to arid rift systems (Bretzler et al., 2011; Furi et al. 2011; Ghiglieri et al, 2012; Siebert et al., 2012; Panno et al., 2013; Forrest et al., 2013; Williams et al., 2013). Stable isotopes (^{2}H, ^{18}O) provide information regarding origins, recharge processes, flow paths and residence times, especially in fractured rock

53 aquifers. Radioactive tracers like tritium (^3H) are relatively accessible methods to estimate groundwater
54 ages and characterize groundwater flow systems. Relatively few studies attempt to quantify mixing
55 between different hydrothermal and cold fluids (Forrest et al., 2013).

56 This study was carried out in the Atemajac-Toluquilla aquifer system (ATAS) which underlies the
57 metropolitan area of Guadalajara, second-most populated city in Mexico (~4.6 million inhabitants), and is
58 located in a complex neotectonic active volcanic system in the Tepic-Zacoalco Rift. Adjacent to this aquifer
59 system is the "La Primavera" caldera. Several survey wells have been drilled up to 3 km deep at La
60 Primavera to explore the potential for geothermal energy (CFE, 2000). Temperatures between 80 and 300
61 °C have been registered in these wells (Verma et al., 2012), and temperatures higher than 40°C have been
62 measured in adjacent springs (Sánchez-Díaz, 2007). The hydrothermal fluids and springs are characterized
63 by high concentrations of Na, Cl, SiO_2, HCO_3, B, F, and TDS. A mixture of hydrothermal fluids and meteoric-
64 derived water has been identified in the springs of "La Primavera" (Sánchez-Díaz, 2007). While it is
65 assumed that this caldera influences the aquifer system underneath the metropolitan area, the
66 proportion of hydrothermal fluids and cold water is not clear. Moreover, nitrate contamination has been
67 related to exogenic processes induced by anthropogenic activity (GEOEX-SIAPA, 2003). The diversity of
68 the chemical results from previous studies has contributed to the difficulty in clearly evaluating the
69 relationship between the fluids (see Results and Discussion section).

70 This study aims to understand the flow dynamics of groundwater by using the combination of statistical
71 and geochemical methods. Water groups and factors that control the groundwater chemical processes
72 were identified using a cluster and principal component analysis. Environmental tracers were used to
73 assess chemical evolution. Mixing proportions of selected fluids in public wells were estimated by means
74 of a multivariate mixing calculation and validated by a chloride mass balance. This study is the first of its
75 kind to report a comprehensive understanding of groundwater flow processes below the Guadalajara

metropolitan area. This information is strategic to decision makers from local water authorities regarding water resources management.

2 Study area

The study area (1368 km^2) is situated in the central portion of the state of Jalisco (Fig. 1). It belongs to the Lerma-Santiago river system, which drains into the Pacific Ocean. The climate according to Köppen is a warm temperate with dry winter “Cwa” (Peel et al., 2007). The National Water Commission reports an average annual temperature of 20.9°C and an average annual precipitation of 904 mm, occurring mostly between May and October. The mean annual evapotranspiration is 712 mm according to Turc formula (CONAGUA, 2010).

2.1 Hydrogeological Settings

The study area is located in the western portion of the Mexican Volcanic Belt (MVB), a 1000 km-long volcanic arc that crosses central Mexico in E–W direction from the Pacific to the Atlantic Ocean. The MVB originated in the Late Miocene in response to the subduction of the Cocos and Rivera plates below the North American plate along the Middle America Trench. The belt has a composition of intermediate to silicic rocks (Alva-Valdivia et al., 2000). The western end of the MVB defines the fault bounded crustal Jalisco Block (Ferrari et al., 2007; Valencia et al., 2013). The northern and eastern boundaries of this block consist of asymmetric continental rifts formed by tilted blocks with escarpments between 800 and 1000m (Zárate-del Valle and Simoneit, 2005); the Tepic–Zacoalco Rift to the north runs in an NW–SE direction, and the Colima Rift to the east runs in an N–S direction; these rifts join the E–W oriented Citala or Chapala Rift in what is known as the Jalisco Triple Junction located 60 km SSW of the city of Guadalajara (Fig. 1). This area is a complex and active neotectonic structure that controls and regulates the development of the rift-floor, limited by normal faults (Michaud et al., 2000; Zárate-del Valle and Simoneit, 2005). The Atemajac and Toluquilla Valleys are located in the lower Tepic–Zacoalco Rift and are bordered by hills,

volcanic cones (El Cuatro, San Martín), plateaus (Tonalá) and volcanic calderas (La Primavera), among other features (Sánchez-Diaz, 2007).

Atemajac and Toluquilla valleys consist of a relatively thin cover of Quaternary lacustrine deposits overlying a thick section of Neogene volcanic rocks including silicic domes, lava and cinder cones, lithic tuffs, basalts, ignimbrites and other pyroclastic rocks, andesites and volcanic breccia, and a basement consisting of Oligocene granite (Campos-Enríquez et al., 2005; Gutiérrez-Negrín, 1988; Urrutia et al., 2000) (Fig. 2). Hydrogeologically, these valleys are underlain by two aquifers (Fig. 3). The upper aquifer consists of alluvial and lacustrine sediments, Pleistocene pre-caldera pyroclastic materials (Tala tuff) such as volcanic ash flows and lapilli, and rhyolitic domes. These sediments represent an unconfined aquifer of up to 450 m thickness with hydraulic conductivities ranging from 1.6×10^{-7} to 2.0×10^{-4} m/s and porosities from 20 to 40% (Sánchez-Díaz, 2007; CONAGUA, 2010). Groundwater recharge sources of this aquifer are rainwater and ascending vertical fluids from the lower aquifer (Gutierrez-Negrin, 1991). Groundwater flows via faults and Toba tuffs in direction to the central and northern portion of the study area. The lower aquifer consists of fractured andesites and basalts from Pliocene, with hydraulic conductivities and porosities ranging from 10^{-8} to 10^{-4} m/s and from 5 to 50%, respectively. This semi-confined to confined aquifer has been related to geothermal fluids (Venegas et al., 1991; GEOEX-SIAPA, 2003). Groundwater of this aquifer flows preferentially in southeastern direction (Ramírez et al., 1982).

Pumping wells are drilled in the upper aquifer. Its water table distribution is shown in Fig. 2. In the Atemajac valley, groundwater flow direction is oriented mainly from southwest to northeast, from the topographically higher areas, towards the Santiago river, with possible recharge from normal faults west from Guadalajara city (Fig. 3, section I and II); while in Toluquilla the flow of groundwater circulates from northwest to southeast (Fig. 3, section III) (GEOEX-SIAPA, 2003; CONAGUA, 2009). However,

anthropogenic activity has been changing the flow paths, resulting in the formation of different cones of depression. The major discharge is given by well pumping activities and springs in the escarpment of the Santiago river (GEOEX-SIAPA, 2003; CONAGUA, 2009 and 2010). Due to the heavy extractions from the aquifer system, water table levels are falling up to 2.2 m/year and 0.3 m/yr on average in Atemajac and Toluquilla aquifers, respectively (GEOEX-SIAPA, 2003). The constructed well depth is up to 500 m and up to 380 m in the valley of Atemajac and Toluquilla, respectively. Depth to water table reaches up to 150 m below ground level in the Atemajac valley and 50 m in Toluquilla valley (GEOEX-SIAPA, 2003).

2.2 Hydrothermal System

The La Primavera caldera, with a diameter of ~10 km, borders the study area to the west. It is a very young (Late Pleistocene) volcanic complex underlain by a magma chamber whose top reaches a depth of 4 km (Verma et al., 2012). Drilling has revealed that the oldest units consist of granitic and granodioritic rocks found mainly at a depth of approximately 3000 m. These rocks are mainly overlain by andesitic rocks approximately 1150 m thick. The third lithologic unit, which is approximately 100 m thick, consists of rhyolites. The uppermost unit is a sequence of lithic tuffs and minor andesite with an average thickness of approximately 750 and 1000 m, respectively (Campos-Enríquez et al, 2005; Urrutia et al., 2000; Verma et al., 2012). The system is characterized by an asymmetric structure with NW-SE regional basalt lineaments that belong to the Tepic Zacoalco Rift and local NE-SW fractures in the upper units extending beneath Guadalajara (Alatorre-Zamora and Campos-Enríquez, 1991; Campos-Enríquez and Alatorre-Zamora, 1998). The temperatures, which were measured at the bottom of exploratory wells that were drilled up to 3 km deep, vary from 80 to 300°C (Verma et al., 2012). It appears that heated meteoric water ascends along fault or fracture zones to near surface depths and supplies springs with temperatures of >40°C (Venegas et al., 1985). The hydrothermal fluids are characterized by very high concentrations of Na (679-810 mg l^{-1}), Cl (865-1100 mg l^{-1}), SiO_2 (943-1320 mg l^{-1}), B (75-150 mg l^{-1}) and TDS (2810-4065 mg l^{-1}) (Maciel-Flores and Rosas-Elguera,1992), while the springs are of Na-Cl-HCO_3 type with relatively high

concentrations of Na (260-331 mg l^{-1}), Cl (85-185 mg l^{-1}), SiO_2 (209-253 mg l^{-1}), HCO_3 (395-508 mg l^{-1}), B (10.8-12.3 mg l^{-1}), F (8.5 mg l^{-1}) and TDS (1071-1240 mg l^{-1}), indicating a mixture between hydrothermal fluids and local rainwater origin with ratios of 1:2 to 1:10 (Gutiérrez-Negrín, 1988; Sánchez-Diaz, 2007).

3 Methods

3.1 Field and laboratory

Water samples were collected from 40 production wells in March 2011 using standard protocols. The samples were analyzed for major and minor ions, trace elements and isotopes (δ^2H, $\delta^{18}O$, ^3H). Field parameters such as temperature, pH, electrical conductivity (EC), and dissolved oxygen (DO), were measured using portable meters (Thermo, Orion). Alkalinity was determined in the field by volumetric titration (0.02N H_2SO_4) of filtered water samples to pH 4.3. At each sampling site, new and pre-rinsed low density polyethylene bottles were filled with filtered (0.45 µm) sample water. Cation and silica samples were acidified with ultrapure HCl to pH<2, and all of the samples were stored in the laboratory at a constant temperature of 4°C. Dissolved cations and anions were determined by inductive-coupled plasma mass spectrometry (ICP-MS) and ion chromatography, respectively. Duplicates of selected samples were analyzed using inductive-coupled plasma optical emission spectrometry (ICP-OES) and ion chromatography, following standard methods (APHA, 2012).

Stable water isotopes were analyzed at Environmental Isotope Laboratory, University of Waterloo, Canada. To conduct deuterium (^2H) analyses, sample water was reduced on hot manganese (512°C) and the released hydrogen was analyzed by GC-MS. To conduct oxygen-18 (^{18}O) analyses, water was equilibrated with CO_2. Preparation and extraction took place on a fully automated system vessel attached to a VG MM 903 mass spectrometer. The ^2H and ^{18}O results are reported as δ-values with respect to the VSMOW (Vienna Standard Mean Ocean Water) standard. Tritium (^3H) was analyzed at Environmental

Isotope Laboratory, University of Arizona, using a liquid scintillation counter after electrolytic enrichment. The average accuracy of tritium analyses was ~0.3 TU.

3.2 Techniques of analysis

A preliminary description of water chemistry and identification of possible processes was performed using a correlation analysis. A hierarchical cluster analysis (HCA) organized samples into classified groups which were evaluated according to their geographic correspondence. A principal component analysis (PCA) elucidated the main controls on groundwater chemistry. All of the statistical calculations were performed using Minitab version 17.1 (Minitab, 2013).

The multivariate mixing and mass balance model, or M3 (Laaksoharju et al., 2008), was used to help to understand groundwater composition. The main aim of M3 is to differentiate between what is due to mixing and what is due to water-rock reactions. The M3 method compares the measured groundwater composition of each sample to the selected reference water and reports the changes in terms of mixing and reactions. A PCA is used to summarize the groundwater data by using the majority of the dissolved groundwater constituents Ca, Na, Mg, K, Cl, SO_4 and HCO_3 in combination with the isotopes δ^2H, $\delta^{18}O$ and ^3H. The outcome of the analyses can be visualized as a scatter plot (PCA plot) for the first two principal components. The observations inside the polygon of the PCA plot are compared to the previously chosen reference water compositions. The mixing calculations create ideal mixing models that use linear distances of the samples from the selected reference waters in the PCA plot.

In this study, the following compositions of samples were used as reference waters: i) three deep wells located in the La Primavera geothermic field and representing hydrothermal water; with data taken from Mahood (1983), Maciel-Flores (1992) and Prol-Ledezma (1995): well PP1 (T=255 °C, Cl=851 mg l^{-1}, B=120 mg l^{-1}, Li=9.9 mg l^{-1} and Na= mg l^{-1}), well PP2 (T=265 °C, Cl=1,120 mg l^{-1}, B=131 mg l^{-1}, Li=8.5 mg l^{-1} and Na=2000 mg l^{-1}), and well PP3 (T=265 °C, Cl=1,500 mg l^{-1}, B=54 mg l^{-1}, Li=3.9 mg l^{-1} and Na=3310 mg l^{-1}); ii)

well AT37 representing local groundwater with low temperature and salinity (Table 1); iii) well AT12 with low temperature and high salinity was taken as polluted reference water (Table 1). Although it is uncertain whether the selected reference waters are end members or close to, they were selected from the available dataset. Well AT37 is an adequate candidate for local groundwater because it is located in the recharge area showing little interaction with rocks. The three deep wells in La Primavera caldera are most probably also an appropriate selection of hydrothermal reference water because their temperatures are in the range of geothermic temperatures according to Verma et al. (2012).

Chloride mass balance was applied with the purpose of validation of the M3 modeling estimates. This method has been discussed and applied in similar environments (e.g. Han et al., 2010) and assumes that extracted groundwater is a mix of two end members (thermal and non-thermal) and that the Cl ion behaves conservative which means that it does not participate in any chemical reactions even at high temperatures.

4 Results and discussion

Sánchez-Diaz (2007) used groundwater temperature and total dissolved solids as criteria to classify wells in hydrothermal water from Toluquilla (HT), hydrothermal water from springs NE of Guadalajara (HG), non-hydrothermal, local groundwater (LG), and mixed groundwater (MG) with both HT and LG (Fig. 4). Considering different sets of historical and new data, this classification is too subjective, especially in the lower TDS range. Furthermore, some inconsistencies between correlation results from different sampling campaigns show that the interpretation is not straightforward. The Mg concentration, for example, decreases with increasing temperature as expected from hydrothermal fluids (Panichi and Gonfiantini, 1981); on the other hand, an increasing Mg trend at low temperatures is observed indicating saline groundwater. Finally, it was not clear if there are different sources of hydrothermal or saline waters that affect the local groundwater. These complications motivated us to use multivariate techniques instead of

commonly used scatterplots and criteria to divide samples into groups and interpret for potential factors/sources. Because the measured parameters varied considerably from study to study, only data from this study were considered for chemical characterization and multivariate analyses.

4.1 Groundwater Chemical Characterization

Table 1 shows the concentrations of measured groundwater chemical elements, field parameters and isotopic data, along with the hydrochemical classification. The classification of waters was performed with HCA using 20 variables (pH, temperature, EC, DO, Na, K, Ca, Mg, Cl, HCO3, SO4, NO3-N, Sr, Si, Fe, F, Zn, ^{3}H, ^{2}H, ^{18}O). With the help of Ward's linkage rule iteratively neighboring points (samples) were linked through a similarity matrix (Ward, 1963). The squared Euclidian distance was selected as the similarity measurement. The second method was a PCA. For both cluster algorithms, lognormal distributed data were previously log-transformed, and all of the variables standardized (z-scores). The HCA samples were classified into 4 major groups as represented by the dendrogram (Fig. 5) and median values (Table 2). The values for Li, Mn and Ba were not considered in the cluster analysis, because most samples had concentrations below the detection limit.

The four groups are plotted on a Piper diagram to demonstrate chemical differences (Fig. 6). Salinity increases as groundwater moves east- and southeastwards from La Primavera field to discharge areas along topographic flow path. EC values reach typically 600 µS cm^{-1} in the discharge areas of urbanized Guadalajara, except for Toluquilla wells where values ascend to 2300 µS cm^{-1}. Group 4 (n=19) is a Na-HCO_3 water type located in recharge zones in the western portion and reflects a short (local) groundwater flow path with poor circulation. It shows low temperatures (average 25.3 °C) and salinity (254 µS cm^{-1}), however elevated NO_3-N (9.1 mg l^{-1}) values, possibly derived from agricultural practices. Groundwater that moves in northern and eastern direction attains a Na-HCO_3 to mixed HCO_3 water type (group 2, n=12), with increased temperatures (30.2 °C) but similar low salinities (300 µS cm^{-1}), indicating water-rock

237 interactions. Groundwater in the discharge area in central Guadalajara city evolves to a Na-SO_4 to mixed
238 HCO_3 water type (group 3, n=3), with higher concentrations of several elements indicating an important
239 impact from anthropogenic pollution, i.e. SO_4 (70.6 mg l^{-1}), NO_3-N (12.4 mg l^{-1}), Na (52.2 mg l^{-1}) and Cl
240 (38.9 mg l^{-1}). Finally, water that moves from recharge zone at Primavera caldera southeast towards the
241 central part of Toluquilla valley, attains a Mg-HCO_3 and mixed HCO_3 type (group 1, n=6). These wells show
242 highest temperatures (33.8 °C) and salinity (EC=1,575 µS cm^{-1}), and lowest NO3-N (0.17 mg l^{-1}) (Fig. 3).

243 This preliminary evaluation of evolution of groundwater chemistry along principal flow paths indicates
244 that groundwater flow is affected by different sources. In the central and northern part of the study area
245 local groundwater from La Primavera caldera undergoes water-rock interactions and mixes with
246 mountain-front recharge as well as return flow from agricultural plots and urban water cycling (Fig. 3,
247 Section I and II), while in the southern portion local water mixes with water from deeper formations that
248 interacts with volcanic rocks of the La Primavera caldera and causes increased mineralization and
249 temperatures (Fig. 3, Section I and II).

250 A factor analysis transformed the 20 variables into a reduced number of factors. The PCA, which loads
251 most of the total variance onto one factor, was used in this study. The factors were extracted through the
252 principal components method. Varimax rotation, where one factor explains mostly one variable, was
253 selected. For fixing the maximum number of factors to be extracted, only factors with eigenvalues higher
254 than one were taken into consideration (Kaiser normalization).

255 Table 3 shows that 4 factors may explain 77% of the variance. Factor 1 (42% of the variance) largely
256 represents high salinity. The correlations of temperature, Na and Cl indicate hydrothermal influence, while
257 HCO_3, Na and Sr could be connected to mineralization and rock dissolution processes, and cationic
258 exchange. In factor 2 (17%) the temperature is inversely related with DO, ^3H, and to a lesser degree, NO_3
259 and SO_4, suggesting that this factor represents water affected by human activities, either urban or

agricultural. In addition, Table 1 and Figure 7 shows that waters affected by human activities are most evaporated. Sulfate could be related to contamination due to the infiltration of commonly applied sulfate-based fertilizers during the rainy season. This occurs because all the wells are undersaturated with regard to gypsum, indicating that the water does not move through deposits of this mineral. In factor 3 (11%) the relationship between ^{2}H and ^{18}O reveals the existence of recharge water. This factor is generated almost entirely by the linear relationship between O and H isotopes. The relation with temperature indicates the recharge conditions at different recharge sites. Factor 4 (7%) may be indicative of dissolution of minerals that contain F. The study of Sánchez-Díaz (2007) indicates that rhyolitic rocks and ashes of the study area are responsible for releasing F. Comparable trends have been observed in various similar volcanic environments in central and northern Mexico (Mahlknecht et al., 2004, Mahlknecht et al., 2008).

4.2 Isotope hydrology

Data from this study and complementary data reported by other investigations (González et al., 1992; GEOEX-SIAPA, 2003) are used to study the origin and evolution of water in the study area (Fig. 7a). The $\delta^{2}H$ vs. $\delta^{18}O$ graph shows that groundwater is of meteoric origin with variable evaporation and mixed with hydrothermal fluid. Although all studies show a similar trend, the data reported by González et al. (1992) registered heavier $\delta^{18}O$ values that may be attributable to evaporation or hydrothermal influence. Similar $\delta^{18}O$ values in thermal systems have been reported in other studies, e.g. El-Fiky (2009) and Stumpp et al. (2014) with $\delta^{18}O$ values ranging from -6.7 to -5.6 ‰ and -4.8 to +0.8 ‰, respectively. Water from group 1 (hydrothermal influenced) collected in Toluquilla, has a narrow range of $\delta^{18}O$ (-9.4 to -8.8‰) and $\delta^{2}H$ (-67 to -68‰) values. They tend to fall slightly below and parallel to the RMWL, possibly indicating different climate conditions during recharge. These samples show isotopic depletion, indicating that recharge by meteoric water is low, as demonstrated by a deuterium excess that ranges from 4 to 8 ‰ with an average of 5.5 ‰ (Fig. 7b). On the other hand, it is possible that only a displacement of $\delta^{18}O$ is occurring, which

283 could correspond to a geothermal effect and mixing with meteoric waters (Giggenbach and Lyon, 1977;
284 Herrera and Custodio, 2003). The increased Cl concentrations compared to other groups evidences
285 mixture with hydrothermal fluids and longer residence times (Fig. 7c). Group 2 waters, collected in the
286 eastern and southern part of the ATAS, have $\delta^{18}O$ and $\delta^{2}H$ values ranging from -9.6 to -8.6‰ and from -
287 63 to -71‰, respectively. These waters fall along the RMWL. Deuterium excess values vary between 5.3
288 and 8.1 ‰ with an average of 6.7 ‰. These values are similar to other groups (Fig. 7b), therefore, in
289 accordance with the low concentration of Cl, groundwater recharge is of meteoric origin (Fig. 7c). Group
290 3 waters (influenced by anthropogenic pollution) are quite different from the rest; they have heavier $\delta^{18}O$
291 values ranging from -7.9 to -5.7‰, and $\delta^{2}H$ values varying from -59.6 to -47.5‰, and are strongly affected
292 by evaporation. Also a lower deuterium excess in the order of +4‰ is observed (Fig. 6b y 6c). The enriched
293 outlier AT12 represents groundwater from a recreational park with lagoons. In this well there is a negative
294 deuterium excess indicating that rainwater presented evaporative diffusion processes in the soil during
295 recharge process (Custodio, 1997; Manzano et al., 2001). Group 4 waters, mostly from La Primavera
296 recharge area, are covering a relative wide range of values compared to group 1 and 2. Their $\delta^{18}O$
297 signatures vary from -10.3 to -8.4‰, and their $\delta^{2}H$ signatures from -72.2‰ to -63.9‰. Deuterium excess
298 in these wells is the highest and indicate preferential recharge during certain times of the year (Jiménez-
299 Martínez and Custodio, 2008). The overlapping of group 1, 2 and 4 indicates that aquifer formations are
300 mostly hydraulically interconnected. Although altitude variations are in the order of only 400 m around
301 La Primavera caldera, this seems to be enough to generate an altitude effect (Fig 7d).

302 Tritium results indicate that groundwater within the study area includes both pre-modern (pre-1950s)
303 and modern recharge. The values range from 0.3 to 3.0 TU which suggests a contribution from modern
304 water in most sampled sites (Table 1). Lowest values are in the order of laboratory analysis accuracy, thus
305 these waters may not contain modern water. The majority of waters with ^{3}H lower than 1.0 TU are in the
306 southern portion of the aquifer system. Elevated ^{3}H values (>1.5 TU) located mostly in the La Primavera

307 volcanic system represent young waters or recent recharge with little mixing of path lines. Waters with
308 ^{3}H values <1.5 TU illustrate that these wells may represent mixing of flow paths with modern and pre-
309 modern groundwater residence times. These waters are found mostly in Toluquilla, corresponding to
310 elevated EC, Cl and DIC values. The mixing of water from different ages is expectable because the aquifer
311 is under unconfined conditions, while wells penetrate the saturated zone to a considerable depth, at times
312 up to 500 m, and are almost always completely screened.

313 ## 4.3 Mixing patterns

314 Using a recommended permissible factor of 0.05 (Laaksoharju et al, 2009), all samples are located inside
315 the cover area of the polygon of PCA plot (Fig. 8). The estimated mixing proportions are present in Table
316 4. Results indicate that the proportions of hydrothermal fluids are largest in group 1 varying from 1.9 to
317 12.5%. The hydrothermal mixing proportions according to Cl mass balance method were consistently
318 higher, ranging from 6.2 to 20.6%. Especiall AT5 shows important differences between both methods. The
319 other groups show hydrothermal fractions below 1.4% according to M3 modeling and 4.4% obtained from
320 Cl mass balance method. The differences between the two methods is not only due to the distinct
321 underlying algorithm of both methods, but also due the fact that M3 modeling uses 3 reference waters
322 and Cl mass balance only 2 reference waters (thermal/non-termal). Group 3 represents an insignificant
323 share of hydrothermal water (~0%) due to fact that these wells are located in recharge areas. On the other
324 hand, this group shows an important proportion of anthropogenic impacted water (>50%), while all other
325 groups are less affected (<37%).

326 These results validate the initial selection of groups based on cluster analysis. Geographically,
327 groundwater with elevated hydrothermal proportions is located in the south to southeastern area
328 (Toluquilla), and elevated proportions of polluted groundwater are located mostly in the urbanized area
329 of Guadalajara. Hydrothermal fractions computed with Cl mass balance method are general higher than

those with M3 program, while for group 3 (fresh groundwater) there is no correspondence between methods. Differences may be due to the underlying conceptual differences in both approaches. However there is a generally high correlation between both methods (r^2 = 0.87) which validates the results.

4.4 Groundwater Flow System of Guadalajara

The hydrogeological Atemajac-Toluquilla system is located in the northeastern area of the Tepic-Zacoalco Rift, a complex and active neotectonic structure. Local groundwater recharge for Atemajac-Toluquilla Valley originates from rainfall mainly over the La Primavera caldera in the central western portion of the study unit. It flows from the upper alluvial sediments towards the valley floor and Santiago River. Recharge water is of Na-HCO3 water type with low temperatures, salinities, Cl and Na values, elevated NO_3 concentrations, as well as relatively high tritium activities in the range of 0.5 -2.9 TU indicating little mixing of flow paths and recent recharge from pristine soils and return flow from agricultural plots, especially in Toluquilla valley. This result confirms also a relatively fast transport through the unsaturated zone (Herrera and Custodio, 2014). As groundwater circulates in northeastern (Atemajac valley) and eastern direction (Guadalajara city) following the hydraulic gradient, its temperature and salinity increases moderately. The wells are typically drilled in Tala tuff underlain by andesites to basaltic andesite rocks. Locally groundwater evolves to a Na-SO_4 to mixed HCO_3 water type, with relatively high contents of SO_4, NO_3, Na, Cl and tritium (~2TU) indicating an important impact from anthropogenic pollution in urban Guadalajara.

Underground heat flow suggests the existence of a magma chamber below the La Primavera caldera, which provides hydrothermal fluids observed on surface expressions such as the La Soledad solfatara and the Cerritos Colorados geothermal field. Regional groundwater that is in contact with these fluids circulates through the lower Atemajac-Toluquilla aquifer specifically below Santa Anita and Toluquilla locations. These Mg-HCO_3 to mixed HCO_3 waters are characterized by elevated temperatures, salinity, Cl,

Na and HCO_3 values, low tritium values (<1.7 TU) and contain considerable concentrations of Li, Mn, B and F, indicating thermal influence, circulation through an active volcanic center and fault zones, and water-rock interactions. The corresponding wells are typically drilled in basalt-andesitic rock formations. The well depth of these wells range from 200 to 300 m and depth-to-water table is about 50 m. The low tritium concentration indicates pre-modern infiltration. Low tritium concentrations in deep wells, according to Herrera and Custodio (2014), are due to a mix of water from the upper aquifer and the vertical ascending flow from the lower aquifer. On the other hand, the tritium values show that geochemically speaking, the water predominates as an old fraction (Custodio, 1989). The isotopic composition of groundwater confirms the interconnectivity between water from deeper and shallow rock materials.

5 Conclusions

This work represents the first time that groundwater flow dynamics of Guadalajara region have been analyzed and characterized by using a suite of statistical and geochemical methods. Geochemical methods have been combined with multivariate statistical analysis and the multivariate mixing and mass-balance model (M3) to determine the mixing patterns of different fluids when considering fresh groundwater, hydrothermal fluids and human impacted waters. The mixing proportions have been compared to estimates from chloride mass balance method.

The initial classification of groundwater groups by cluster analysis has been confirmed by water isotopic technologies, and identifying the controlling factors by principle component analysis is consistent with M3 modeling. The origin of groundwater recharge and the mixture of fresh groundwater with hydrothermal fluids and polluted water components was identified. A conceptual flow model was constructed for the Atemajac-Toluquilla aquifer system. The local flow is associated with the infiltration of rainwater that occurs at higher altitudes. Hydrothermal waters are probably related to recharge outside the study area and upward vertical flow in the La Primavera caldera and the valley of Toluquilla. TDS, Cl, Na, Mn and Li,

are most indicative of hydrothermal fluids. Modern water polluted with SO_4 and NO_3 can be associated with infiltration of urban sewage and agricultural return flow. According to M3 modeling, the proportion of hydrothermal fluids within older waters was between 1.9% and 12.5%, whereas it was lower than 1.4% within other waters. The proportion of polluted water in groundwater reached up to 52% in urbanized areas.

M3 is a powerful tool to evaluate the mixing proportions of selected reference waters present in aquifers. We recommend the use of the suite of traditional methods, environmental tracers, statistical analysis and M3 modeling in other aquifers with potentially multiple groundwater origins, especially in active volcanic systems where mixing is an important process. One limitation with this approach, however, is the representativeness of selected reference waters and samples. Part of this uncertainty may be overcome by repeating the field campaign considering seasonal/time variations.

These outcomes may help water authorities to identify wells with hydrothermal mixture or polluted water and act accordingly. The information regarding the proportions of fresh groundwater, hydrothermal fluids and polluted waters in each well indicates that the contaminants can be attributed to source waters. For example, Li, Mn, Ba, F and As can be associated with hydrothermal fluids, and SO_4 and NO_3 are related to the production or use of fertilizers, dyes, glass, paper, soaps, textiles, fungicides or insecticides. These results helps authorities to decide whether certain wells have to be isolated or closed in order to provide Guadalajara with the required drinking water quality.

Acknowledgments

This work was financially supported by Fundación FEMSA and the Chair for Sustainable Water Use (Tecnológico de Monterrey). Fundación FEMSA had no role in study design, data collection and analysis,

decision to publish, or preparation of the manuscript. We would like to thank R. Ledesma and A. Mazón for their assistance in the field work and graphical edition.

References

Ako, A. A., Eyong, G. E. T., Shimada, J., Koike, K., Hosono, T., Ichiyanagi, K., Akoachere, R., Tandia, B. K., Nkeng, G. E., and Ntankouo, N. R.: Nitrate contamination of groundwater in two areas of the Cameroon Volcanic Line (Banana Plain and Mount Cameroon area), Appl. Water Sci., 4, 99-113, 2013.

Aksoy, N., Simsek, C., and Gunduz, O.: Groundwater contamination mechanism in a geothermal field: a case study of Balcova, Turkey, J. Contam. Hydrol., 103, 13-28, 2009.

Alatorre-Zamora, M. A. and Campos-Enríquez J. O.: La Primavera Caldera (Mexico): Structure inferred from gravity and hydrogeological considerations, Geofis. Int., 31, 371-382, 1991.

Alva-Valdivia, R., Goguitchaichvili, A., Ferrari, L., Rosas-Helguera, J., Urrutia-Fucugauchi, J., and Zambrano-Orozco, J. J.: Paleomagnetic data from the Trans-Mexican Volcanic Belt: Implications for tectonics and volcanic stratigraphy, Earth Planets Space, 52, 467-478, 2000.

APHA.: Standard Methods for examination of water and wastewater, 22nd ed., Washington: American Public Health Association, 2012.

Appelo, C. A. J. and Postma, D.: Geochemistry, groundwater and pollution (2nd ed.): Leiden, The Netherlands, A.A. Balkema, 649 p., 2005.

Bretzler, A., Osenbrück, K., Gloaguen, R., Ruprecht, J. S., Kebede, S. and Stadler, S.: Groundwater origin and flow dynamics in active rift systems e a multi-isotope approach in the Main Ethiopian Rift, J. Hydrol., 402, 274-289, 2011.

Campos-Enríquez, J. O. and Alatorre-Zamora, M. A.: Shallow crustal structure of the junction of the grabens of Chapala, Tepic-Zacoalco and Colima, Mexico, Geofis. Int., 37, 263-282, 1998.

Campos-Enríquez, J. O., Domínguez-Méndez, F., Lozada-Zumaets, M., Morales-Rodríguez, H. F., and Andaverde-Arredondo, J. A.: Application of the Gauss theorem to the study of silicic calderas: the calders of La Primavera, Los Azufres, and Los Humeros (Mexico), J. Volcanol. Geotherm. Res., 147, 39-67, 2005.

CFE - Comisión Federal de Electricidad (2000): Geotermia. Gerencia de Geotermia, 23 pp.

Chiodini, G., Marini, L., and Russo, M.: Geochemical evidence for the existence of high temperature hydrothermal brines at Vesuvio volcano, Italy, Geochim. Cosmochim. Acta, 65, 2129-2147, 2001.

CONAGUA - Comisión Nacional del Agua: Determinación de la Disponibilidad de Agua en el Acuífero Atemajac-Toluquilla), Estado de Jalisco (Determination of Water Availability in the Atemajac-Toluquilla aquifer, Jalisco state. México, D.F., 2010.

CONAGUA - Comisión Nacional del Agua: Determinación de la Disponibilidad de Agua en el Acuífero Toluquilla, Estado de Jalisco (Determination of Water Availability in the Toluquilla aquifer, Jalisco state. México, D.F., 2009.

Custodio, E.: Groundwater characteristics and problems in volcanic rock terrains. Isotope Techniques in the Study of the Hydrology of Fractured and Fissured Rock, in: Proceedings of an Advisory Group Meeting, Vienna, Austria, 17-21 November 1986, 87-137, 1989.

Custodio, E.; Llamas, M. R., and Samper, J.: La evaluación de la recarga a los acuíferos en la planificación hidrológica, Asociación Internacional de Hidrogeólogos, Grupo Español-Instituto Tecnológico Geominero de España, 1997.

De Vries, J. J. and Simmers, I.: Groundwater recharge: an overview of processes and challenges, Hydrogeol. J. 10, 5-17, 2002.

Di Napoli, R., Aiuppa, A., Bellomo, S., Brusca, L., D'Alessandro, W., Gagliano Candela, E., Longo, M., Pecoriano, G., and Valenza, M.: A model for Ischia hydrothermal system: evidences from the chemistry of thermal groundwaters, J. Volcanol. Geotherm. Res., 186, 133-159, 2009.

Di Napoli, R., Martorana, R., Orsi, G., Aiuppa, A., Camarda, M., De Gregorio, S., Gagliano Candela, E., Luzio, D., Messina, N., Pecoraino, G., Bitetto, M., de Vita, S., and Valenza, M.: The structure of a hydrothermal system from an integrated geochemical, geophysical and geology approach: The Ischia Island case study, Geochem. Geophys. Geosyst., 12, 1-25, 2011.

Dogdu, M. S. and Bayari, C. S.: Environmental impact of geothermal fluids on surface water, groundwater and streambed sediments in the Akarcay Basin, Turkey, Environ. Geol., 47, 325-340, 2005.

Edmunds, W. and Smedley, P.: Residence time indicators in groundwater: the East Midlands Triassic sandstone aquifer, Appl. Geochem., 15, 737-752, 2000.

El-Fiky, A.: Hydrogeochemistry and Geothermometry of Thermal Groundwater from the Gulf of Suez Region, Egypt, J. King Abdulaziz Univ. Sci., 20, 71-96, 2009.

Evans, W. C., Sorey, M. L., Cook, A. C., Kennedy, B. M., Shuster, D. L., Colvard, E. M., White, L. D., and Huebner, M. A.: Tracing and quantifying magmatic carbon discharge in cold groundwaters: lessons learned from Mammoth Mountain, USA, J. Volcanol. Geotherm. Res., 114, 291-312, 2002.

Ferrari, L., Valencia-Moreno, M., and Bryan, S.: Magmatism and tectonics of the Sierra Madre Occidental and its relation with the evolution of the western margin of North America, in: Geology of México: Celebrating the Centenary of the Geological Society of México, edited by: Alaniz-Álvarez, S.A. and Nieto-Samaniego, A.F., Geol. Soc. Am., Special Paper, 422, 1-39, 2007.

460 Forrest, M. J., Kulongoski, J. T., Edwards, M. S., Farrar, C. D., Belitz, K., and Norris, R. D.: Hydrothermal
461 contamination of public supply wells in Napa and Sonoma Valleys, California. Appl. Geochem., 33, 25-
462 40, 2013.

463 Furi, W., Razack, M., Abiye, T. A., Kebede, S., and Legesse, D.: Hydrochemical characterization of complex
464 volcanic aquifers in a continental rifted zone: the Middle Awash basin, Ethiopia, Hydrogeol. J., 20, 385-
465 400, 2011.

466 GEOEX-SIAPA.: Estudio geohidrológico Atemajac-Toluquilla, Sistema Intermunicipal de Agua Potable y
467 Alcantarillado (SIAPA), Guadalajara, Jalisco, México, 2003

468 Ghiglieri, G., Pittalis, D., Cerri, G., and Oggiano, G.: Hydrogeology and hydrogeochemistry of an alkaline
469 volcanic area: the NE Mt. Meru slope (East African Rift-Northern Tanzania), Hydrol. Earth. Syst. Sci., 16,
470 529-541, 2012.

471 Giggenbach, W. F. and Lyon, G. L.: The chemical and isotopic composition of water and gas discharges
472 from the Ngawha geothermal field, Northland, DSIR, Chem. Div. Report No: CD:30/555/7, 1977.

473 Goff, F. and Janik, C. J.: Geothermal systems, in: Encyclopedia of Volcanoes, edited by: Sigurdsson, H.,
474 Houghton, B., McNutt, S., Rymer, H., and Stix, J., Academic Press, San Diego, CA, 817-834, 2000.

475 González, H. L., Mata, A. I., Sánchez, D. L. F.: Estudio isotópico e hidroquímico de los acuíferos de
476 Toluquilla-Ocotlán-La Barca, en el estado de Jalisco, Informe técnico, Instituto Mexicano de Tecnología
477 del Agua, 1992.

478 Gutiérrez-Negrín, L. C. A.: Recursos Geotérmicos en La Primavera, Jalisco, Ciencia y Desarrollo, 16, 57-69,
479 1991.

480 Gutiérrez-Negrin, L.: La Primavera, Jalisco, Mexico: geothermal field, Transactions of the Geothermal
481 Research Council, 12, 161-165, 1988.

Han, D. M., Liang, X., Jin, M. G., Currell, M. J., Song, X. F., and Liu, C.M.: Evaluation of groundwater hydrochemical characteristics and mixing behavior in the Daying and Qicun geothermal systems, Xinzhou Basin, J. Volcanol. Geotherm. Res., 189, 92-104, 2010.

Henley, R. W. and Ellis, A. J.: Geothermal systems, ancient and modern: a geochemical review, Earth. Sci. Rev., 19, 1-50, 1983.

Herrera C. and Custodio, E.: Hipótesis sobre el origen de la salinidad de las aguas subterráneas en la isla de Fuerteventura, Archipiélago de Canarias, España, Bol. Geol. Min., 114, 433-52, 2003.

Herrera, C. and Custodio, E.: Groundwater flow in a relatively old oceanic volcanic island: The Betancuria area, Fuerteventura Island, Canary Islands, Spain. Sci. Total. Environ., 496, 531-550, 2014.

Hockstein, M. P. and Browne, P. R. L.: Surface manifestations of geothermal systems with volcanic heat sources, in: Encyclopedia of Volcanoes, edited by: Sigurdsson, H., Houghton, B., McNutt, S., Rymer, H., and Stix, J., Academic Press, San Diego, CA, 835-856, 2000.

Jiménez-Martínez, J. and Custodio E.: El exceso de deuterio en la lluvia y en la recarga a los acuíferos en el área circum-mediterránea y en la costa mediterránea española, Boletín Geológico y Minero, 119, 21-32, 2008.

Laaksoharju, M., Skårman, E., Gómez, J.B., and Gurban, I.: M3 version 3: user's manual. SKB TR-09-09. Stockholm, Sweden: Svensk Kärnbränslehantering AB; 2009.

Laaksoharju, M., Smellie, J., Tullborg, E-L., Gimeno, M., Molinero, J., Gurban, I., and Hallbeck, L.: Hydrogeochemical evaluation and modelling performed within the site investigation programme, Appl. Geochem, 23, 1761-1795, 2008.

Maciel-Flores, R. and Rosas-Elguera, J.: Modelo geológico y evaluación del campo geotérmico La Primavera, Jal., México, Geofís. Int., 31, 359-370, 1992.

504 Mahlknecht, J., Horst, A., Hernández-Limón, G., and Aravena, R.: Groundwater geochemistry of the
505 Chihuahua City region in the Rio Conchos Basin (Northern Mexico) and implications for water resources
506 Management, Hydrol. Process., 22, 4736-4751, 2008.

507 Mahlknecht, J., Steinich, B., and Navarro de León I.: Groundwater chemistry and mass transfers in the
508 Independence aquifer, central Mexico, by using multivariate statistics and mass-balance models,
509 Environ. Geol, 45, 781-95, 2004.

510 Mahood, G. A., Truesdell, A. H. and Templos M. L. A.: A reconnaissance geochemical study of La Primavera
511 geothermal area, Jalisco, Mexico, J. Volcanol. Geotherm. Res., 16, 247-261, 1983.

512 Manzano, M., Custodio, E., Loosli, H., Cabrera, M. C., Riera, X., and Custodio, J.: Palaeowater in coastal
513 aquifers of Spain, in: Palaeowaters in Coastal Europe: Evolution of Groundwater since the Late
514 Pleistocene, edited by: Edmunds, W.M. and Milne, C.J., Geological Society of London: Special
515 Publication, 189: 107-138, 2001.

516 Michaud, F., Gasse, F., Bourgois, J., and Quintero, O.: Tectonic controls on lake distribution in the Jalisco
517 Block area (western Mexico) from Pliocene to Present, in: Cenozoic Tectonics and Volcanism of Mexico,
518 edited by: Delgado-Granados, H., Aguirre-Díaz, G.J., and Stock, J.M., Geol. Soc. Am., Special paper, 334,
519 99-110, 2000.

520 Minitab (2013). Statistical Software (versión 17.1). MINITAB® and all other trademarks and logos for the
521 Company's products and services are the exclusive property of Minitab Inc. All other marks referenced
522 remain the property of their respective owners.

523 Navarro, A., Font, X., and Viladevall, M. Geochemistry and groundwater contamination in the La Selva
524 geothermal system (Girona, Northeast Spain), Geothermics, 40, 275-285, 2011.

525 Panichi, C. and Gonfiantini, R.: Geothermal waters, in: Stable Isotope Hydrology, edited by: Gat, J.R. and
526 Gonfiantini, R., IAEA Tech. Rep. Ser., 241-272, 1981.

527 Panno, S. V., Hackley, K. C., Locke, R. A., Krapac, I. G., Wimmer, B., Iranmanesh, A., and Kelly, W.R.:
528 Formation waters from Cambrian-age strata, Illinois Basin, USA: Constraints on their origin and
529 evolution based on halide composition, Geochim. Cosmochim. Ac., 122, 184-197, 2013.

530 Peel, M.C., Finlayson B. L., McMahon T.A.: Updated world map of the Koppen-Geiger climate classification,
531 Hydrol. Earth Syst. Sci., 11, 1633–1644, 2007

532 Prol-Ledesma, R. M., Hernandez-Lombardini, S. I., and Lozano-Santa Cruz, R.: Chemical variations in the
533 rocks of La Primavera geothermal field (Mexico) related with hydrothermal alteration, in: Proceedings
534 of the 17th NZ Geothermal Workshop, Auckland, New Zealand, 8-10 November 1995, 47-53, 1995.

535 Ramírez, S. G., Casco del Razo, J. y Mata, V. V. M.: Hidrología regional de la zona geotérmica de la
536 Primavera-San Marcos-Hervores de la Vega, Jal. Informe técnico (inédito), Comisión Federal de
537 Electricidad, 1982.

538 Reimann, C., Bjorvatn, K., Frengstad , B., Melaku, Z., Tekle-Haimanot, R., and Siewers, U.: Drinking water
539 quality in the Ethiopian section of the East African Rift Valley I—data and health aspects, Sci. Total.
540 Environ., 311, 65-80, 2003.

541 Rozanski, K., Araguás-Araguás, L., and Gonfiantini, R.: Isotopic patters in modern global precipitation, in:
542 Climate Change in Continental Isotopic Records, edited by: Swart, P.K., Lohmann, K.C., McKenzie, J.,
543 and Savin, S., American Geophysical Union, doi: 10.1029/GM078p0001, 1993.

544 Sánchez-Díaz, L. F.: Origen, transporte, distribución y concentraciones de los fluoruros en el sistema
545 hidrogeológico volcánico Atemajac-Toluquilla, Jalisco, México, Ph.D. thesis, Universidad Nacional
546 Autónoma de México, 128 pp., 2007.

Siebert, C., Rosenthal, E., Möller, P., Rödiger, T., and Meiler, M.: The hydrochemical identification of groundwater flowing to the Bet She'an-Harod multiaquifer system (Lower Jordan Valley) by rare earth elements, yttrium, stable isotopes (H, O) and Tritium, Appl. Geochem, 27, 703-714, 2012.

Stumpp, C., Ekdal, A., Gönenc, I. E., and Maloszewski, P.: Hydrological dynamics of water sources in a Mediterranean lagoon, Hydrol. Earth. Syst. Sci., 18, 4825-4837, 2014.

Urrutia F. J., Alva-Valdivia, L. M., Rosas-Elguera, J., Campos-Enriquez, O. Goguitchaichvili, A., Soler-Arechalde, A. M., Caballero-Miranda, C., Venegas Salgado, S., and Sanchez-Reyes, S.: Magnetostratigraphy of the volcanic sequence of Río Grande de Santiago-Sierra de la Primavera region, Jalisco, western Mexico, Geofis. Int., 39, 247-265, 2000.

Valencia, V. A., Righter, K., Rosas-Elguera, J., Lopez-Martinez, M., and Grove, M.: The age and composition of the pre-Cenozoic basement of the Jalisco Block: implications for and relation to the Guerrero composite terrane, Contrib. Mineral. Petrol., 166, 801-824, 2013.

Venegas, S. S., Ramírez, S. G., Romero, G. C., Reyes, V. P., Razo, M. A., Gutiérrez, N. L. C. A., Arellano, G. F. and Rerezyera, Z. J.: La Primavera geothermal field, Jalisco, in: The Geology of North America, edited by: Salas, G.P., Economic Geology, Mexico. The Geological Society of America, 1991.

Venegas, S., Herrera, J. J., and Maciel, F. R.: Algunas características de la Faja Volcánica Mexicana y de sus recursos geotérmicos, Geofis. Int., 24, 47-83, 1985.

Verma, S. P., Arredondo-Parra, U. C., Andaverde, J, Gómez-Arias, E., and Guerrero-Martínez, F. J.: Three-dimensional temperature field simulation of a cooling of a magma chamber, La Primavera caldera, Jalisco, Mexico, Int. Geol. Rev., 54, 833-843, 2012.

Ward, J. H.: Hierarchical grouping to optimize an objective function, J. Am. Stat. Assoc., 58, 236-244, 1963.

568 Wassenaar, L. I., Van Wilgenburg, S. L., Larson, K., and Hobson, K. A.: A groundwater isoscape (δD, $\delta^{18}O$)
569 for Mexico, J. Geochem. Explor., 102, 123-36, 2009.

570 Williams, A. J., Crossey, L. J., Karlstrom, K. E., Newell, D., Person, M., and Woolsey, E.: Hydrogeochemistry
571 of the Middle Rio Grande aquifer system - Fluid mixing and salinization of the Rio Grande due to fault
572 inputs, Chem. Geol., 351, 281-298, 2013.

573 Zarate-del Valle, P. F. and Simoneit, B. R. T.: La generación de petróleo hidrotermal en sedimentos del
574 Lago Chapala y su relación con la actividad geotérmica del rift Citala en el estado de Jalisco, Rev. Mex.
575 Cienc. Geol., 22, 358-370, 2005.

576

577 # Table Captions

578 Table 1: Concentrations of measured field parameters, groundwater elements, isotopic data, and
579 hydrochemical classification. Data are given in mg l^{-1}, except otherwise indicated. Note: T = temperature,
580 DO = dissolved oxygen, EC = electrical conductivity, Bal. = ion balance error, S.U. = standard units

581 Table 2: Median values of water chemistry of the groundwater subgroups determined from HCA. Data are
582 given in mg l^{-1}, except where otherwise indicated.

583 Table 3: Rotated component matrix of the factor analysis for groundwater samples from the Atemajac
584 Toluquilla aquifer system. Coefficients between -0.1 and 0.1 are suppressed. Note: DO = dissolved oxygen,
585 T = temperature, EC = electrical conductivity.

586 Table 4: Mixing proportions from the multivariate mixing and mass-balance model, M3, using the
587 following reference waters: deep wells PP1, PP2 and PP3 as a reference for hydrothermal fluids; no. 12 as
588 a reference for polluted water; and no. 37 as reference for fresh groundwater, and hydrothermal mixing

589 proportions based on Cl mass balance calculations. Note: Avg = average obtained from calculation using
590 the three different hydrothermal reference waters; SD=standard deviation.
591
592
593
594

Figure Captions

Figure 1: Location of study area (black area) in Mexico and tectonic structures of western Central Mexico.

Figure 2: Surface geology, water table distribution and location of wells sampled in the study area. Note: GMA = Guadalajara metropolitan area

Figure 3: Cross-sections indicated in Fig. 2 and considering hydrogeological settings and water types of selected wells.

Figure 4: Plot of water temperature vs. total dissolved solids for different groundwater collecting campaigns in the study area. The delimitation of classified wells according to Sánchez-Díaz (2007) is also shown. Note: HT=hydrothermal water from Toluquilla, HG=hydrothermal water from springs NE of Guadalajara, LG=local groundwater, MG = mixed groundwater (HT and LG).

Figure 5: Dendrogram showing HCA classification with groups and subgroups of samples of the Atemajac-Toluquilla aquifer system. The dashed line indicates the ‘‘phenon line’’, an arbitrary line that defines subgroups.

Figure 6: Piper diagram of groundwater samples from the Atemajac-Toluquilla aquifer system with well groups.

Figure 7: (a) Deuterium and oxygen-18 in groundwater from the ATAS using this and previous studies. Note: GMWL = Global Meteoric Water Line (Rozanski et al., 1993), RMWL = Regional Meteoric Water Line (Wassenaar et al., 2009); (b) oxygen-18 vs. deuterium excess with labelled altitudes; (c) oxygen-18 vs. chloride concentration; and (d) oxygen-18 vs. altitude.

Figure 8: PCA plots of the M3 model from mixing of hydrothermal fluids with cold groundwater and polluted waters.

Table 1:

ID	Well name	Well depth (m)	pH (S.U.)	T (°C)	EC (uS cm^{-1})	DO	Na	K	Ca	Mg	Cl	HCO_3	SO_4	NO_3-N	Sr	SiO_2	Fe	F	Zn	Li	Mn	Ba	^3H (TU)	^2H (‰)	^{18}O (‰)	Bal (%)	Water type
AT1	Toluquilla 1	300	7.3	25	345	5.34	44.2	6.8	13.3	4.9	9.4	146.4	21.5	3.8	0.07	44	0.05	0.95	0.040	0.06	<0.01	0.05	1.70	-64.3	-8.6	-4	Na-Ca-HCO3
AT2	Toluquilla 6	300	7.0	25	1619	5.76	152.0	58	28.9	103	70.1	1068.8	6.5	<0.04	0.38	38.5	0.14	0.33	0.066	0.33	0.26	0.5	0.70	-68.4	-9.3	-8	Mg-Na-HCO3
AT3	Toluquilla 17	200	7.0	25	2310	5.25	114.0	36	58.7	92.9	82.4	1031.3	5.0	0.07	0.45	35.1	0.18	0.65	0.018	0.33	0.51	0.32	0.70	-66.5	-8.8	-10	Mg-Na-HCO3
AT4	Toluquilla 22	300	7.0	31.8	1792	5.1	147.0	40.9	89.7	113	85.4	1415.2	6.6	<0.04	0.61	53.6	0.05	0.99	0.076	0.37	0.22	0.26	1.20	-67.4	-9.1	7	Mg-Na-HCO3
AT5	Toluquilla 7	230	7.0	36.4	1900	5.48	174.0	48.4	80.7	104	229.0	697.6	22.4	<0.04	0.52	61.6	0.37	3.50	0.088	0.47	0.83	0.39	0.40	-66.5	-8.9	3	Mg-Na-HCO3-Cl
AT6	Las Pintas	250	7.2	33.6	718	6.21	102.0	33.9	31.2	16	14.5	435.2	5.9	0.03	0.32	40	0.04	0.26	0.023	<0.05	0.04	0.08	0.90	-64.7	-8.8	6	Na-HCO3
AT7	Garabatos	200	6.8	25	188.9	6.73	16.1	1.2	2	0.4	2.2	24.4	9.7	4.53	0.01	22.8	0.03	1.01	0.020	<0.05	<0.01	<0.02	2.20	-70.5	-9.6	2	Na-HCO3-SO4
AT8	Santa Ana Tepetitlan	250	6.9	25.8	240.4	6.02	38.5	2.3	5.8	1	30.6	18.3	34.6	71.6	0.01	45.3	0.02	3.79	0.005	0.08	<0.01	<0.02	0.60	-71.5	-9.9	9	Na-NO3-Cl-SO4
AT9	Tapatíos 1	258	6.2	25	310	6.61	57.3	7.2	6.7	2.3	3.7	122.0	12.3	4.68	0.02	52.6	0.03	0.97	0.224	0.09	<0.01	<0.02	1.20	-71.1	-9.8	9	Na-HCO3
AT10	Topacio	235	6.7	21.8	569	6.34	63.8	21	14.3	6.3	5.2	242.2	8.9	0.42	0.1	38.4	0.03	0.84	0.092	<0.05	<0.01	0.05	0.90	-65.2	-8.9	13	Na-Ca-Mg-HCO3-SO4-Cl
AT11	Jardines del Bosque	250	7.1	27.8	309	5.75	26.5	3.5	7.8	2.6	14.0	30.5	29.4	5.76	0.03	29.8	0.02	0.46	0.046	<0.05	<0.01	0.04	2.10	-63.9	-8.4	12	Na-Mg-Ca-HCO3
AT12	Agua Azul	40	7.1	29.1	354	3.3	44.1	8.9	23	7.4	50.3	24.4	95.2	11.8	0.12	41.4	0.02	0.20	0.005	<0.05	<0.01	<0.02	2.40	-47.5	-5.7	0	Na-Mg-Ca-HCO3
AT13	Educadores Jalisc.	300	6.5	32.8	1111	3.93	14.6	6.3	16.8	4.8	1.3	102.5	1.1	0.43	0.12	35	0.02	0.21	0.161	<0.05	<0.01	<0.02	0.50	-67.0	-9.1	7	Na-Mg-HCO3
AT14	Tanque Tesistán	292	7.1	32.5	325	4.22	23.3	6	5.1	2.6	4.8	58.6	7.1	1.12	0.04	22.9	0.02	0.72	0.092	<0.05	<0.01	<0.02	1.00	-64.4	-8.8	7	Na-Ca-HCO3
AT15	Górgoros	80	7.4	30.6	231.7	6.5	38.4	4.5	4.2	1.3	11.0	78.1	25.2	5.40	0.02	48.6	0.03	0.81	0.198	<0.05	<0.01	<0.02	1.50	-65.6	-9.0	-5	Na-Ca-Mg-HCO3
AT16	Fray Pedro	70	7.3	30	334	4.28	21.0	6.5	4.6	2.2	5.6	68.3	8.5	1.43	0.03	20.1	0.02	0.34	0.095	<0.05	<0.01	<0.02	0.30	-62.4	-8.7	9	Na-Mg-HCO3
AT17	Bajo La Arena B	80	8.7	24.6	218.5	4.32	20.8	2.8	1.8	0.5	0.7	53.7	2.2	2.40	0.01	48.3	0.04	1.40	0.584	<0.05	<0.01	<0.02	0.90	-72.2	-9.9	4	Na-Mg-Ca-HCO3
AT18	S. Juan de Ocotán 1	120	7.9	22.5	345	4.95	27.1	8.5	4.5	4.2	2.0	87.8	1.5	0.05	0.02	25.6	0.04	2.49	0.132	<0.05	<0.01	<0.02	0.70	-67.1	-9.4	8	Na-Ca-HCO3-SO4
AT19	Manantial Toluquilla	--	8.3	24.6	143.9	5.8	57.5	13.4	25	12.6	35.6	87.8	65.7	13.8	0.18	38.2	0.07	0.57	0.308	<0.05	<0.01	0.13	2.00	-59.2	-7.9	-1	Na-HCO3-F
AT20	La Estancia 4	150	7.7	23.6	382	2.42	39.1	9.4	13.3	8.6	3.3	162.7	2.5	0.41	0.16	37.7	0.19	0.32	0.294	<0.05	<0.01	0.03	0.40	-67.0	-9.4	12	Na-Ca-HCO3
AT21	La Loma de S. Juan	60	7.5	25.3	569	4.4	38.3	8.6	16.7	12.9	7.2	172.2	6.1	0.95	0.18	44.3	0.03	0.46	0.963	<0.05	<0.01	<0.02	0.80	-67.8	-9.5	5	Na-Mg-Ca-HCO3
AT22	Rancho Alegre	150	7.7	27.5	213.9	4.5	92.6	28.5	37.3	47.8	41.5	467.9	19.6	0.80	0.47	46.6	0.06	0.94	0.397	0.16	0.13	0.12	0.50	-66.3	-9.3	1	Na-HCO3
AT23	Mimbela	50	6.9	28.2	445	5.02	55.0	10.3	18.5	6.1	30.7	97.6	50.8	11.7	0.09	43.4	0.03	0.22	0.008	<0.05	<0.01	0.03	1.90	-59.6	-7.9	-3	Na-HCO3
AT24	Tesistan 14	120	7.0	25.1	305	6.34	33.9	3.5	3.8	1.3	3.1	126.9	13.5	4.20	0.02	45.4	0.05	0.37	0.020	0.06	<0.01	<0.02	1.90	-68.8	-9.6	7	Na-Ca-SO4-HCO3-Cl
AT25	Fovisste	200	6.8	24.4	649	6.68	18.4	7.8	3.1	1.7	1.8	43.9	6.7	2.08	0.02	44.2	0.03	0.35	0.035	<0.05	<0.01	<0.02	0.80	-69.2	-9.5	5	Na-Ca-SO4-Cl
AT26	Power Center	90	7.5	32.6	190.7	5.65	35.3	6.1	7.5	2.7	2.1	113.7	8.6	1.58	0.04	41.9	0.05	0.24	0.033	<0.05	<0.01	<0.02	1.60	-68.3	-9.5	4	Ca-Na-Mg-HCO3
AT27	Virreyes	300	6.8	29.4	363	4.81	43.9	7.2	5	3.2	1.1	146.4	1.5	0.73	0.02	51.6	0.12	1.16	0.113	0.06	<0.01	<0.02	0.80	-70.9	-10.0	5	Na-HCO3
AT28	Tesistan 61	275	6.7	24.6	222.4	5.94	27.0	4.4	4	1.6	1.4	83.0	3.5	2.07	0.02	47.8	0.35	0.39	0.431	<0.05	<0.01	<0.02	1.60	-69.4	-9.7	1	Na-HCO3-SO4
AT29	Tesistan 56	270	6.9	33.7	298	7.66	16.7	1.7	7.1	2.1	7.6	30.5	21.0	6.75	0.01	19.1	0.02	0.22	0.019	<0.05	<0.01	<0.02	1.70	-66.5	-9.3	6	Na-HCO3
AT30	Tesistan 70	250	7.1	26	107.8	4.83	20.0	8.8	7	1.9	2.9	60.8	12.3	5.72	0.07	47.5	0.03	0.390	0.048	<0.05	<0.01	<0.02	1.70	-67.8	-9.4	-1	Na-HCO3
AT31	Unid. Dep. Tonala	118	6.7	29.8	351	3.5	40.3	12.7	13.3	7.6	3.4	181.8	1.7	1.06	0.14	35.2	0.06	0.26	0.112	<0.05	<0.01	<0.02	0.70	-65.6	-9.0	13	Na-HCO3
AT32	San Ismael	285	6.7	23.9	451	4.37	20.2	7.5	15.8	7.8	0.3	132.2	0.2	0.05	0.17	33.6	0.03	0.06	0.100	<0.05	<0.01	0.03	0.70	-64.8	-8.8	15	Na-Ca-HCO3-SO4-Cl
AT33	Tateposco 2	250	6.8	25.5	192.1	5.46	44.5	13.4	12.6	8	6.3	166.4	2.4	0.7	0.14	35.9	0.03	0.34	0.130	<0.05	<0.01	<0.02	0.70	-64.5	-8.9	-15	Na-HCO3
AT34	El Lindero	55	6.7	26.6	138.9	6.57	22.2	7.4	8.5	5.5	1.2	97.6	6.1	2.02	0.11	40.8	0.03	0.18	0.182	<0.05	<0.01	0.03	2.00	-68.9	-9.6	4	Na-HCO3
AT35	Vivero Los Amigos	24	6.6	27.3	234.7	7.72	19.9	16.6	10.1	4.1	2.7	53.7	40.1	25.4	0.08	30.9	0.02	0.03	0.070	<0.05	<0.01	<0.02	2.90	-64.5	-9.4	5	Na-HCO3
AT36	El Taray	200	6.4	24.7	242	4.37	11.5	7.8	9.3	4.7	0.5	102.5	0.3	0.12	0.04	36	0.03	0.26	0.341	<0.05	<0.01	<0.02	0.70	-67.1	-9.3	3	Na-HCO3
AT37	Viveros del Sur	54	6.3	27.7	160.3	5.63	14.1	0.6	1.9	0.3	2.1	29.3	2.1	1.19	0.01	20.3	0.14	4.90	0.084	<0.05	0.02	<0.02	0.50	-71.6	-10.3	2	Na-HCO3
AT38	Las Pomas	115	6.2	26.4	310	5.74	33.9	1.8	13.5	2.4	9.5	78.1	21.2	5.94	0.02	27.3	0.02	1.67	1.040	0.08	<0.01	<0.02	1.80	-68.5	-9.5	4	Na-Ca-HCO3-SO4
AT39	Potrero La Ordeña	64	6.7	25	165.9	5.93	31.9	8.8	13.2	8.2	10.1	97.6	23.4	17.7	0.15	25.5	0.03	1.25	0.065	<0.05	<0.01	<0.02	1.00	-68.3	-9.4	-22	Na-Ca-HCO3
AT40	Los Gigantes	62	8.0	31.6	182.8	5.65	30.9	2.7	4.7	1.3	2.8	58.6	6.9	4.87	0.02	38.3	0.02	1.71	0.252	0.06	<0.01	<0.02	0.50	-70.4	-9.6	-6	Na-Ca-Mg-HCO3

Table 2:

Group	N	Parameter	pH (S.U.)	T (|C)	EC (uS cm-1)	TDS	DO	^{3}H (TU)	$\delta^{2}H$ (‰)	$\delta^{18}O$ (‰)	HCO_3	K	Mg	Si	Ca	Fe	Na	Sr	Zn	F	Cl	NO_3-N	SO_4	Li	Ba	Mn
1	6	Average	6.9	33.8	1575	733	5.4	0.73	-66.65	-9.02	852.7	41.0	79.5	45.9	54.4	0.14	130.3	0.46	0.11	1.11	87.2	0.17	11.0	0.29	0.28	0.33
		Median	7.0	33.6	1706	710	5.4	0.70	-66.52	-8.98	864.5	38.5	98.0	43.3	48.0	0.10	130.5	0.46	0.07	0.80	76.3	0.05	6.5	0.33	0.29	0.24
2	12	Average	7.2	30.2	300	95	4.5	0.66	-66.09	-9.10	128.0	9.2	5.9	33.6	10.9	0.04	31.2	0.10	0.23	0.67	3.5	0.97	3.9	0.01	0.04	0.01
		Median	7.1	29.9	317	89	4.4	0.70	-66.27	-9.07	117.4	8.2	5.6	35.6	13.0	0.03	29.0	0.11	0.13	0.34	3.3	0.57	2.4	0.00	0.03	0.01
3	3	Average	6.8	23.4	556	229	4.7	2.1	-55.5	-7.2	69.9	10.9	8.7	41.0	22.2	0.04	52.2	0.13	0.11	0.3	38.9	12.4	70.6	0.00	0.08	0.01
		Median	6.7	23.9	569	241	5.0	2.0	-59.2	-7.9	87.8	10.3	7.4	41.4	23.0	0.03	55.0	0.12	0.01	0.2	35.6	11.8	65.7	0.00	0.08	0.01
4	19	Average	7.0	25.3	254	84	6.0	1.5	-68.5	-9.5	75.5	5.4	2.5	38.6	6.6	0.06	29.4	0.04	0.17	1.1	6.2	9.1	15.5	0.02	0.04	0.01
		Median	6.8	25.0	235	77	5.9	1.6	-68.8	-9.5	78.1	4.5	2.1	44.0	6.7	0.03	27.0	0.02	0.07	0.8	2.9	4.5	12.3	0.00	0.04	0.01

621 **Table 3:**

Variable	PC1	PC2	PC3	PC4
pH				0.47
T	0.24	0.23	0.29	
EC	0.32			
DO		-0.25		
^{3}H		-0.37		0.15
^{2}H			0.45	-0.20
^{18}O			0.45	
HCO_3	0.32			
K	0.32			
Mg	0.33			
SiO_2				-0.23
Ca	0.32			
Fe				-0.37
Na	0.33			
Sr	0.32			0.13
Zn				
F				-0.371
Cl	0.3			
NO_3		-0.40		
SO_4		-0.50		
Eigenvalue	8.43	3.38	2.21	1.34
% of variance	42	17	11	7
Cum. % variance	42	59	70	77

622

623 ***Table 4:***

Well ID	Well group	M3 calculations						Cl m-b calculations	
		% fresh groundwater		% polluted water		% hydrothermal water		% hydrothermal water	
		Avg	SD	Avg	SD	Avg	SD	Avg	SD
2	1	78.1	0.6	17.0	0.1	4.9	0.7	6.2	1.4
3	1	68.1	0.7	26.4	0.1	5.5	0.7	7.3	1.7
4	1	73.6	0.7	21.3	0.1	5.1	0.8	7.6	1.7
5	1	63.1	2.0	24.4	0.2	12.5	2.2	20.6	4.8
6	1	67.7	0.0	30.4	0.0	1.9	0.0	1.1	0.3
22	1	75.6	0.3	21.4	0.0	3.0	0.3	3.6	0.8
10	2	71.1	0.1	28.5	0.0	0.4	0.1	0.3	0.1
33	2	69.5	0.1	29.8	0.0	0.7	0.1	0.4	0.1
18	2	80.3	0.1	19.0	0.0	0.7	0.1	0.0	0.0
40	2	89.0	0.0	10.2	0.0	0.8	0.0	0.1	0.0
14	2	68.3	0.1	31.2	0.0	0.6	0.1	0.2	0.1
16	2	62.6	0.1	36.1	0.0	1.2	0.1	0.3	0.1
13	2	76.1	0.1	22.5	0.0	1.4	0.1	0.0	0.0
32	2	69.0	0.1	30.4	0.0	0.7	0.1	0.0	0.0
36	2	78.9	0.1	20.1	0.0	1.1	0.1	0.0	0.0
21	2	82.7	0.0	16.5	0.0	0.9	0.0	0.5	0.1
31	2	72.3	0.1	26.4	0.0	1.3	0.1	0.1	0.0
20	2	80.4	0.1	19.3	0.0	0.3	0.1	0.1	0.0
12	3	0.0	0.0	100.0	0.0	0.0	0.0	4.4	1.0
19	3	48.2	0.0	51.8	0.0	0.0	0.0	3.1	0.7
23	3	48.8	0.0	51.0	0.0	0.1	0.0	2.6	0.6
1	4	66.3	0.0	33.7	0.0	0.0	0.0	0.7	0.2
15	4	73.4	0.0	26.6	0.0	0.0	0.0	0.8	0.2
11	4	63.0	0.0	36.8	0.0	0.2	0.1	1.1	0.2
38	4	84.8	0.0	15.2	0.0	0.0	0.0	0.7	0.2
39	4	82.9	0.0	16.7	0.0	0.3	0.0	0.7	0.2
7	4	89.7	0.0	10.1	0.0	0.2	0.0	0.0	0.0
29	4	78.4	0.0	21.4	0.0	0.2	0.0	0.5	0.1
34	4	86.7	0.0	13.3	0.0	0.0	0.0	0.0	0.0
35	4	75.8	0.0	24.2	0.0	0.0	0.0	0.1	0.0
9	4	93.1	0.0	6.6	0.0	0.3	0.0	0.1	0.0
25	4	85.9	0.1	13.8	0.0	0.4	0.1	0.0	0.0
24	4	86.5	0.0	13.5	0.0	0.1	0.0	0.1	0.0
26	4	84.1	0.1	15.5	0.0	0.4	0.1	0.0	0.0
30	4	82.3	0.0	17.7	0.0	0.0	0.0	0.1	0.0
17	4	96.2	0.0	3.3	0.0	0.5	0.0	0.0	0.0
27	4	95.2	0.0	4.8	0.0	0.0	0.0	0.0	0.0
28	4	88.4	0.0	11.1	0.0	0.5	0.0	0.0	0.0
8	4	93.8	0.2	4.5	0.0	1.7	0.3	2.6	0.6
37	4	100.0	0.0	0.0	0.0	0.0	0.0	0.0	0.0

624

625

626 **Figure 1:**

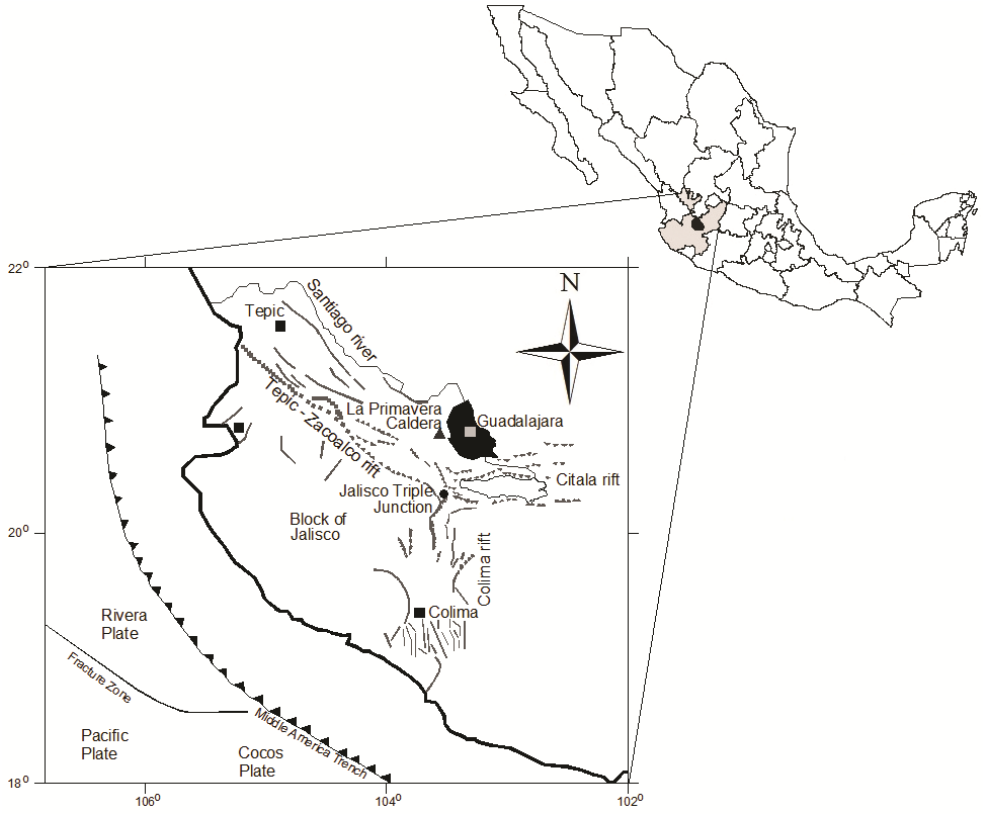

627

628 **Figure 2:**

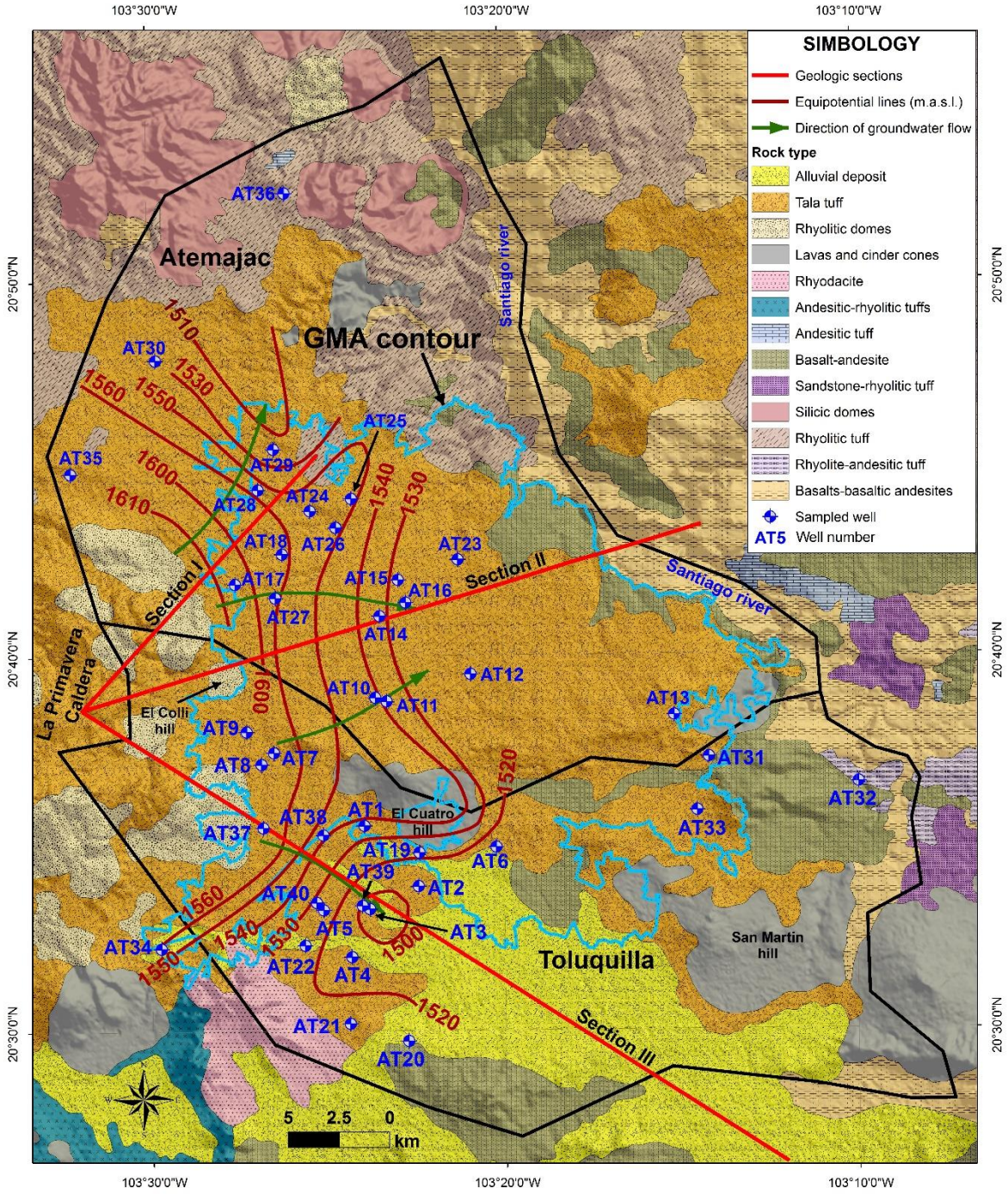

629

630 **Figure 3:**

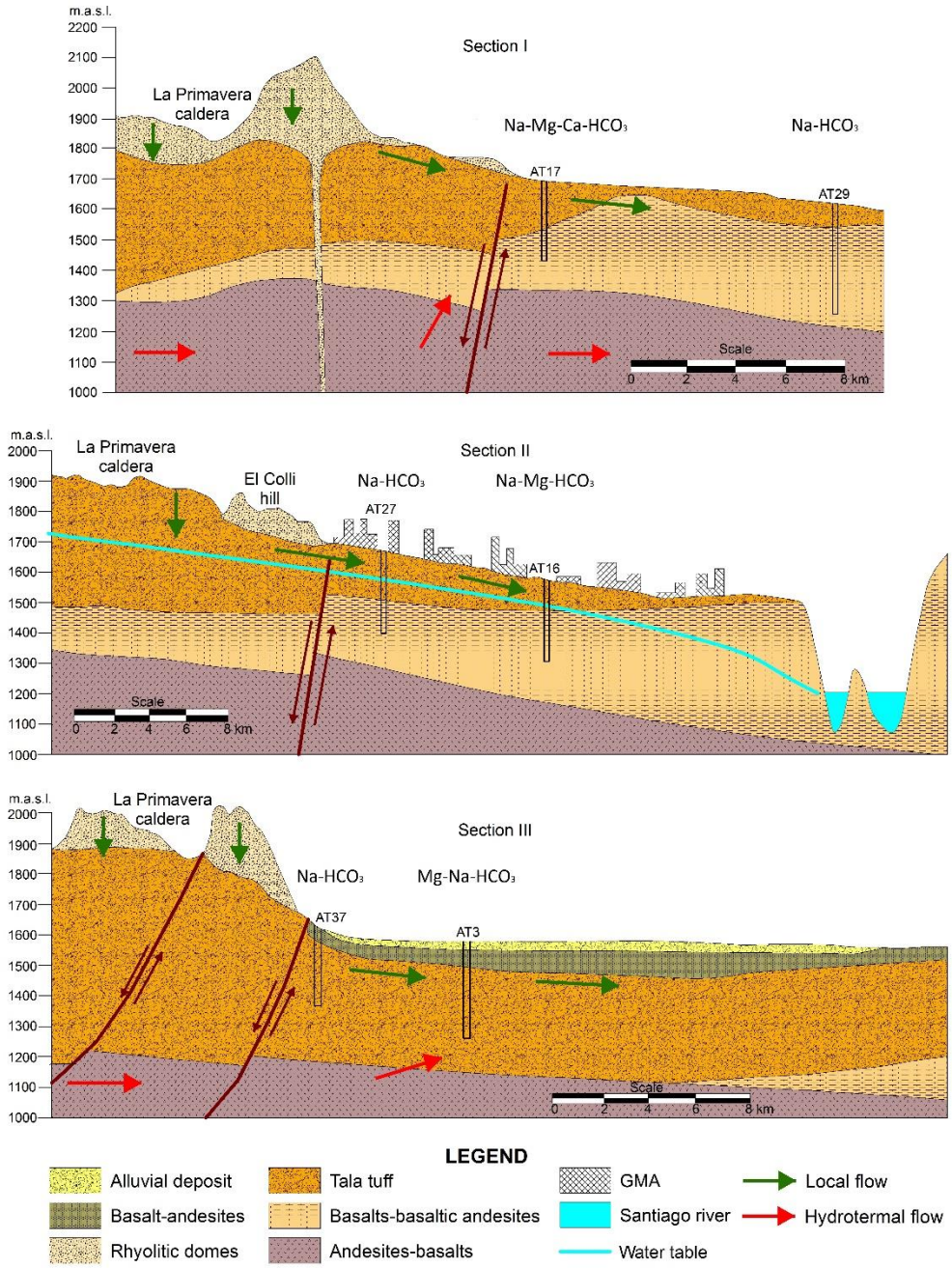

631

Figure 4:

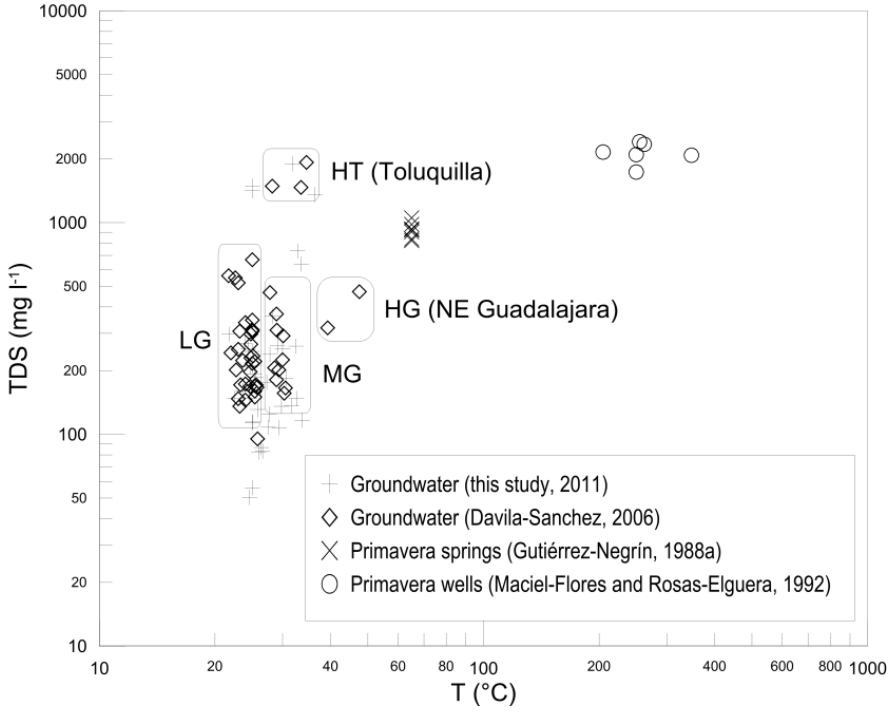

Figure 5:

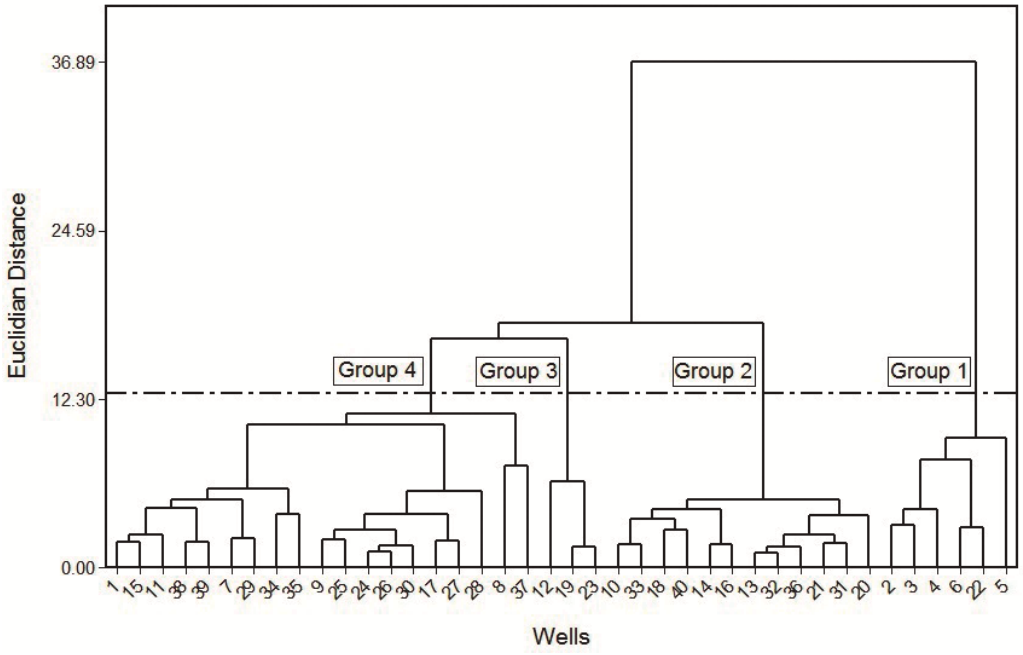

637 **Figure 6:**

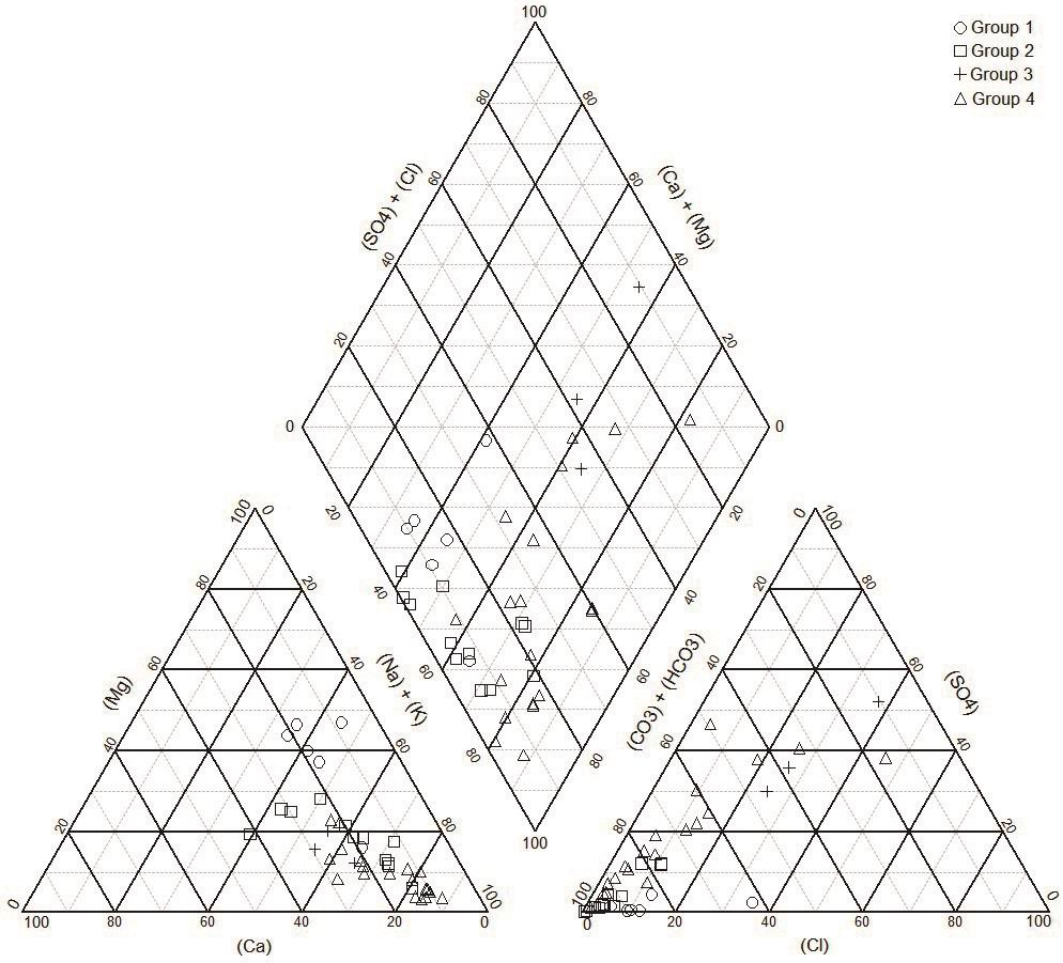

638

Figure 7:

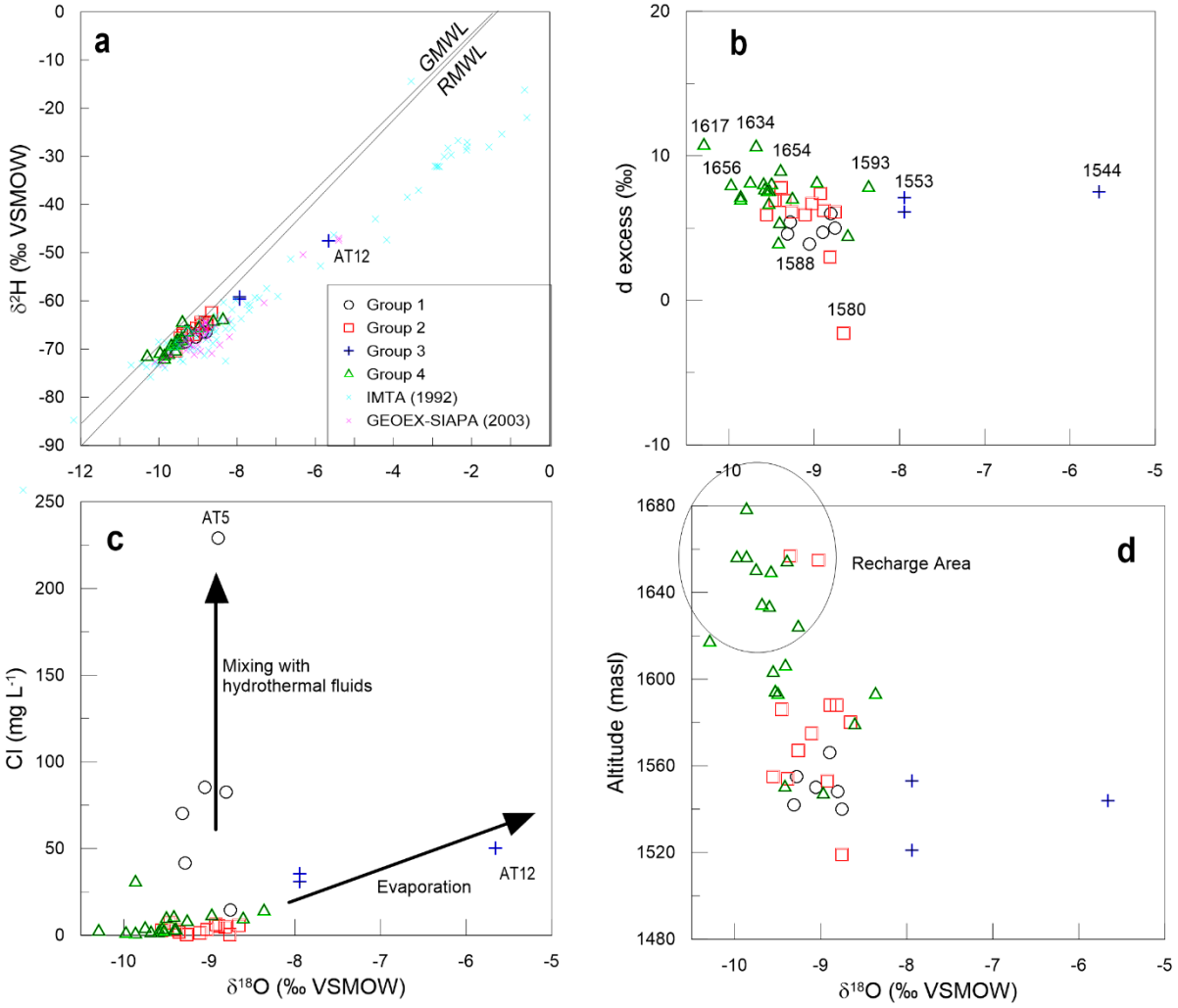

Figure 8: